



Cite this: *Nanoscale*, 2015, 7, 16508

## Large area nanoscale metal meshes for use as transparent conductive layers†

Yuanhao Jin,<sup>a,b</sup> Qunqing Li,<sup>\*a,b</sup> Mo Chen,<sup>a,b</sup> Guanhong Li,<sup>a,b</sup> Yudan Zhao,<sup>a,b</sup> Xiaoyang Xiao,<sup>a,b</sup> Jiaping Wang,<sup>a,b</sup> Kaili Jiang<sup>a,b</sup> and Shoushan Fan<sup>a,b</sup>

We report on the experimental realization of using super-aligned carbon nanotubes (SACNTs) as etching masks for the fabrication of large area nanoscale metal meshes. This method can easily be extended to different metals on both rigid and flexible substrates. The as-fabricated metal meshes, including the ones made of gold, copper, and aluminum, are suitable for use as transparent conductive layers (TCLs). The metal meshes, which are similar to the SACNT networks in their dimensional features of tens of nanometers, exhibit compatible performance in terms of optical transmittance and sheet resistance. Moreover, because the metal meshes are fabricated as an integrated material, there is no junction resistance between the interconnected metal nanostructures, which markedly lowers their sheet resistance at high temperatures. The fabrication of such an effective etching mask involves a simple drawing process of the SACNT networks prepared and a common deposition process. This approach should be easy to extend to various research fields and has broad prospects in commercial applications.

Received 7th July 2015,  
Accepted 2nd September 2015

DOI: 10.1039/c5nr04528b

[www.rsc.org/nanoscale](http://www.rsc.org/nanoscale)

Transparent conductive layers (TCLs) that exhibit both high electrical conductivity and optical transparency are used in many optoelectronic devices like light-emitting diodes (LEDs),<sup>1,2</sup> touch-screen displays,<sup>3</sup> and solar cells.<sup>4,5</sup> The unique properties of the materials in TCLs allow light to pass through them while extracting electrical carriers at the same time. Currently, doped metal oxide films such as tin-doped indium oxide (ITO) and fluorine-doped tin oxide (FTO) are the most common TCLs.<sup>6,7</sup> However, these materials have several important drawbacks, such as the scarcity of indium, brittleness and a relatively high material cost.<sup>8</sup>

Nanomaterials such as carbon nanotubes (CNTs), graphene, metal nanowires and metal meshes show enormous potential for use as TCLs.<sup>9–13</sup> Among these materials, metal meshes may be suitable for replacing ITO.<sup>2</sup> Considerable efforts to improve the transparency and conductivity of metal meshes have been made by many groups.<sup>14–17</sup> However, the

fabrication of such kinds of structures often challenges the limits of traditional techniques, making it really difficult for large-scale product manufacturing at a low cost.

Recently, some new techniques have been used to fabricate metal meshes at high throughput, such as a fiber template,<sup>18</sup> self-assembly at liquid interfaces,<sup>19</sup> and the crackle template.<sup>20</sup> Randomly arranged metal nanowires can be obtained through solution-based processes and used to produce TCLs at a relatively low cost on rigid and flexible substrates.<sup>9</sup> However, such solution-based methods still face some problems, including the difficulty of fine tuning optical transmission and electrical conductivity, contact resistance between the nanowires, and non-uniform distribution of metal nanostructures on the substrate.<sup>20</sup> In general, metal nanowires are only fabricated randomly on a substrate because of the isotropy in the solution environment. Furthermore, the solution environment and related subsequent processes are usually not fully compatible with current semiconductor fabrication processes. More importantly, for touch-screen and solar-cell applications, metal meshes with suitable periodicity possess advantages over randomly arranged nanowires. This is because the relationship between optical transparency and electrical conductivity can be tuned effectively by adjusting the aperture ratio and metal thickness of metal meshes with controllable structures.<sup>2,14</sup>

In this study, super-aligned multi-walled carbon nanotube (SACNT) networks are used as etching masks to fabricate metal meshes *via* reactive ion etching (RIE) for use as TCLs. SACNT networks coated with metal oxides have been proved as

<sup>a</sup>State Key Laboratory of Low-Dimensional Quantum Physics, Department of Physics & Tsinghua-Foxconn Nanotechnology Research Center, Tsinghua University, Beijing 100084, China

<sup>b</sup>Collaborative Innovation Center of Quantum Matter, Beijing, China.

E-mail: QunqLi@mail.tsinghua.edu.cn; Fax: +86 10 62792457;

Tel: +86 10 62796019

† Electronic supplementary information (ESI) available: Microscopy images of Al and Cu metal meshes as fabricated with and without a laser process, resistance and transmittance characterization of Al and Cu metal meshes, microscopy images of the SACNT film with various laser process conditions, resistance characterization of Al and Cu metal meshes against heating temperatures. See DOI: 10.1039/c5nr04528b

an effective way to fabricate metal meshes. Using this approach, the excellent quasi-periodical morphology of the SACNT networks can be transferred to the corresponding metal meshes. With the dimensional features of tens of nanometers, metal meshes exhibit high performance in terms of optical transmittance or sheet resistance and can be easily prepared on rigid or flexible substrates. More importantly, based on the foundation of the commercialized production of SACNT networks, methods for metal mesh preparation are proposed, which make the large-scale fabrication of periodical metal nanomeshes possible for the first time.

As an inexpensive macroscopic material system that is suitable for mass production, SACNT networks have received attention from electrical, optical and mechanical researchers.<sup>21–23</sup> SACNT networks can be used as TCL materials in touch-screen panels. Touch-screen panels based on SACNT networks have been fabricated at the industrial scale and commercialized for use in cell phones and laptops.<sup>24–27</sup> However, because the carrier density of carbon materials is relatively low, the resistance of SACNT networks is thousands of ohms. The junctions between CNTs also increase the resistance of SACNT networks. Further lowering of resistance has only been realized at the cost of transmittance. Therefore, the use of SACNT networks in LEDs and photovoltaics is greatly restricted because the resistance of TCL materials strongly affects the performance of devices.

## Results and discussion

To overcome the shortcomings of TCL materials based on SACNT networks, we decided to convert the fibers in SACNT networks into metal nanowires, which should increase the carrier density compared with that of carbon materials. The process used to fabricate metal meshes from SACNT networks is outlined in Fig. 1(a). A SACNT film was pulled out from a CNT array with a height of 300  $\mu\text{m}$  grown on a four-inch silicon wafer (Fig. 1(b)).<sup>20</sup> SACNT film fabrication can be performed automatically and continuously. In addition, the wafer could be extended to an eight-inch silicon substrate, which guarantees that SACNT films could be prepared conveniently in large quantities at a relatively low cost.<sup>28</sup> The SACNT films were cross-stacked on a metal frame to form SACNT networks. A SEM image of a SACNT network is depicted in Fig. 1(c). The CNTs in each SACNT film were parallel and formed quasi-periodical nanostructures. It is easier to control the transmittance and resistance of TCL materials by the adjustment of period and line density in such an ordered structure than in one with a random distribution of CNTs or metal nanowires.

CNTs have been used as masks in some etching or irradiation processes.<sup>29,30</sup> However, the use of CNTs as masks has been very limited because pure CNTs are not durable towards the etching or irradiation process in most cases, which is one of the main difficulties to generalize this technique in the fabrication of nanopatterned structures. To overcome this shortcoming, we deposited  $\text{Al}_2\text{O}_3$  with a thickness of

10 nm on the SACNT networks by e-beam deposition, to increase the endurance of naked SACNT networks during the RIE process, especially when Ar and  $\text{O}_2$  plasma are involved in metal etching. With the great advantage that SACNT networks are prepared by suspending, CNTs will be coated completely by the metal oxide to ensure the role of masks in RIE. Fig. 1(d) shows a TEM image of a CNT with a 10 nm thick layer of  $\text{Al}_2\text{O}_3$  deposited on it. This image illustrates that the CNTs in the SACNT networks could be totally coated with  $\text{Al}_2\text{O}_3$ . The resulting system should be a stable mask during RIE because no carbon is exposed. An  $\text{Al}_2\text{O}_3$  thickness of 10 nm was used because it was the minimum thickness to completely cover the CNTs, and a thicker  $\text{Al}_2\text{O}_3$  layer would have a negative influence on the etching resolution.

The as-fabricated SACNT networks were then transferred to a substrate coated with 10 nm of Au deposited by e-beam deposition. An alcohol was applied to the interface between the SACNT networks and the Au layer to make the CNTs shrink and encourage the CNTs to bind more strongly with the Au-coated substrate. The transparent substrate materials used in these experiments were rigid glass, flexible polyethylene terephthalate (PET) and scotch tape.

The dimensional features of the SACNT networks were completely transferred to the 10 nm thick Au layer after RIE, using Ar and  $\text{O}_2$  plasma (Ar, 26 sccm;  $\text{O}_2$ , 7 sccm; 10 Pa, 50 W, forward bias voltage 20 kV). Parallel Au nanowires with the morphology of the SACNT networks were formed on the substrate. The transfer process of nanostructures does not require a solution environment. Compared with the current technique for fabricating metal meshes using liquid acid corrosion, the resolution of metal nanostructures obtained *via* RIE was higher and better guaranteed. Furthermore, the SACNT networks act as a mask effectively, so photolithography is not needed, which greatly improves the fabrication efficiency and reduces the cost.

To further investigate the etching process, the substrate before and after etching was compared. Fig. 2(a) shows the morphology of some CNTs in a SACNT network on the deposited Au layer. Because of the limitation of the deposition process and thinness of the Au layer, its surface was fairly rough and it appeared grainy on the micro scale. An AFM image of the same area is presented in Fig. 2(c). In the area where two CNTs cross, a junction was formed and the diameter distribution of CNTs could be verified. Fig. 2(e) displays the corresponding heights measured for three random points in the CNT networks. The CNTs coated with 10 nm of  $\text{Al}_2\text{O}_3$  were around 25 nm high in these local areas, while the diameter of a naked CNT was usually around 10–20 nm.

A SEM image of the same area of the Au layer after etching in Ar and  $\text{O}_2$  plasma and CNT removal is shown in Fig. 2(b). A comparison with Fig. 2(a) reveals that the SACNT networks acted as a mask during the etching process, allowing the dimensional features of the CNTs to be transferred to the Au layer. Au nanowires with the shape and morphology of the CNTs were formed on the substrate. In the areas of the substrate without the CNT mask, the deposited Au was com-

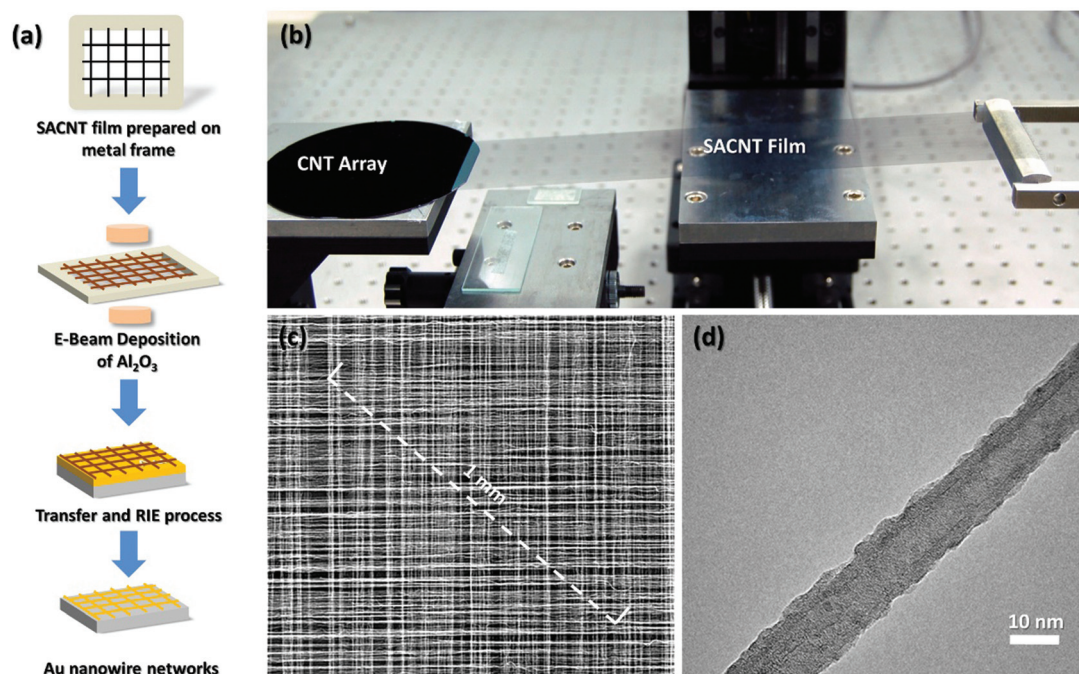


**Fig. 1** (a) Schematic illustration of the process used to fabricate metal meshes from SACNT networks. (b) Photograph showing the fabrication of a SACNT film from a four-inch silicon wafer. (c) SEM image of cross-stacked SACNT films. (d) TEM image of a CNT coated with 10 nm of  $\text{Al}_2\text{O}_3$ .

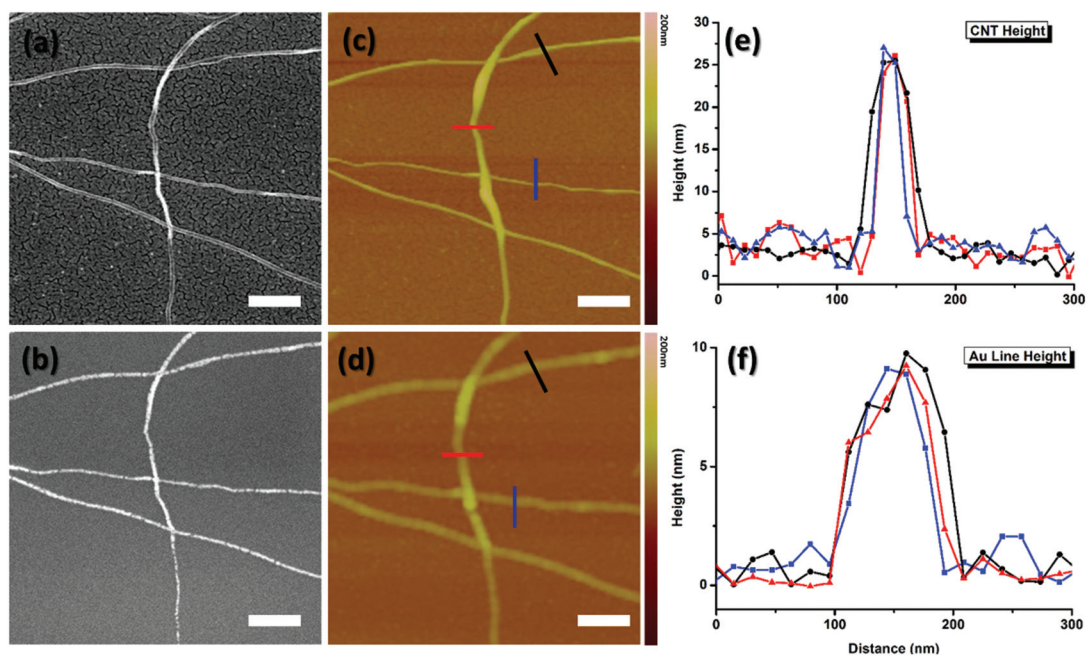


**Fig. 2** SEM images of (a) CNTs on the surface of the deposited Au layer and (b) the corresponding Au nanowires. AFM images of (c) CNTs on the surface of the deposited Au layer and (d) the corresponding Au nanowires. Height of lines measured from the AFM images of (e) CNTs and (f) Au nanowires at three random positions. The scale bars in (a–d) are all 300 nm.

pletely etched away and a grainy surface was no longer observed. In the AFM image of the as-fabricated Au nanowires (Fig. 2(d)), height measurements were taken at the same posi-

tions as in Fig. 2(b); the results are plotted in Fig. 2(f). All of the Au nanowires possessed a height of 10 nm, which was consistent with the thickness of the deposited Au layer. The SEM

and AFM images of the Au nanowires reveal that there are no junctions between the Au nanowires and they are assembled as an interconnected network over a large area. For metal meshes fabricated by methods based on bottom-up or solution processes, the junction resistance between nanowires usually dominates their electrical performance.<sup>9</sup> In contrast, the interconnected metal mesh fabricated here from a single Au layer using the SACNT network mask should avoid the problem of junction resistance.

The SEM image in Fig. 3(a) shows the morphology of the as-fabricated metal mesh. The morphology of the SACNT networks was transferred completely to the Au layer, so integrated Au nanowires were fabricated. A microscopy image of an Au metal mesh on the millimeter scale is shown in Fig. 3(b), in which the morphology of CNTs transferred to the Au layer over a large area could be clearly observed. Such metal meshes have several attractive characteristics as TCLs. First, the SACNT networks could be fabricated over a very large area at a relatively low cost. In addition, it has been proven that SACNTs can be effective and reliable in commercial applications.<sup>24</sup> This should facilitate application of the etching technology developed here in actual products. Second, as mentioned above, the

metal mesh was integrated without any junctions between the nanowires because of the utilization of the top-down etching method, which should lower the resistance of the whole system. Third, the technology used here is fully compatible with standard semiconductor fabrication processes without any material preparation in the solution environment. The correlative methods have also been proved effective in the preparation of semiconductor materials.<sup>32</sup>

To evaluate the performance of the Au metal meshes as TCLs, their transmittance spectra in the visible range (400–800 nm) were measured. Au metal meshes were fabricated on glass substrates from deposited Au layers of different thicknesses. In each case, the height of the as-fabricated Au metal mesh nanowires was consistent with the thickness of the deposited Au layer. As illustrated in Fig. 3(c), the transmittance of the meshes decreased as the thickness of the Au layer increased. At the wavelength of 550 nm, the transmittance of the Au metal mesh fabricated from a 10 nm Au layer was 76%, while it was 65%, 61% and 53% for the meshes fabricated from Au layers with thicknesses of 15, 20 and 25 nm, respectively. At the same time, as the transmittance of the meshes decreased, so did their resistance. The sheet resistances were

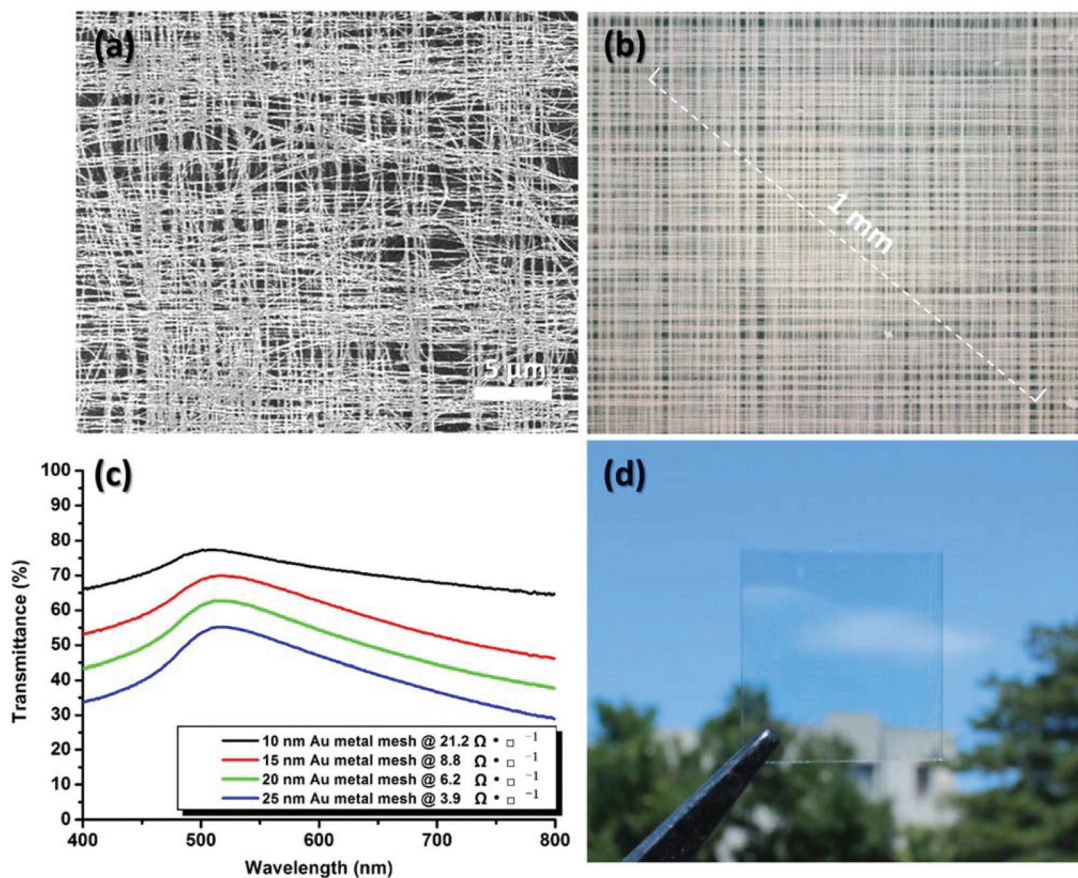


**Fig. 3** (a) SEM and (b) microscopy images of an Au metal mesh fabricated from an Au layer with a thickness of 10 nm. (c) Optical transmittance as a function of wavelength for Au metal meshes on glass substrates. The metal meshes were fabricated from Au layers with thicknesses of 10, 15, 20 and 25 nm. (d) Photograph of an Au metal mesh with a transmittance of 76% at 550 nm on a glass substrate fabricated from a 10 nm thick Au layer.

21.2, 8.8, 6.2 and 3.9  $\Omega \square^{-1}$  for the meshes obtained from Au layers with thicknesses of 10, 15, 20 and 25 nm, respectively. The resistance of each mesh was measured by the four-terminal method over a sample area of 5 × 5 cm using measurement probes with a diameter of 80  $\mu\text{m}$  and a distance between them of 1 mm. Average resistances were calculated based on the results obtained from different positions of the samples and the uncertainty was 1–3 percent, which could indicate the sample resistance in a real situation.

In theory, the sheet resistance of a nanopatterned metallic film could be calculated from  $R_{\text{sq}} = (\rho/h)(a/w)$ , where  $\rho$  is the metal resistivity,  $h$  is the wire thickness and  $(a/w)$  is the duty ratio of the structures.<sup>14</sup> Here, the value of the metal resistivity of gold is assumed as  $\rho_{\text{Au}} = 2.4 \times 10^{-8} \Omega \text{ m}$  to evaluate the sheet resistance.<sup>33</sup> As shown in the microscopy and SEM image, the duty ratio was approximately  $(a/w) = 8$ , where  $w$  is the line width and  $a$  is the period. For the case of  $h = 10 \text{ nm}$ , the typical theoretical value of sheet resistance for the Au metal mesh could be calculated as  $R_{\text{sq}} = 19.2 \Omega \square^{-1}$ . We can see that the experimental result (21.2  $\Omega \square^{-1}$ ) was quite close to the theoretical value, which means that excellent conductivity could be obtained from the as fabricated Au metal meshes in a large area using this method. The excellent results of the experimental resistivity which almost approach the theoretical limits come from the fact that the metal mesh was integrated without any junctions between the nanowires because of the utilization of the top-down etching method, different from the methods when TCL is fabricated from randomly arranged metal nanowires. Similar to ITO and other TCL materials, there was competition between transmittance and sheet resistance in the meshes. These results also demonstrate that the fabrication method developed here can provide TCL materials with various transmittances and sheet resistances simply by changing the thickness of the deposited Au layer. Therefore, Au metal meshes with different transmittances suited for specific applications could be fabricated without any additional steps. The transmittance of the Au metal mesh fabricated from an Au layer with a thickness of 25 nm exhibited a peak at around 500 nm, which made the sample appear pale green. This is because the Au layer with a thickness of tens of nanometers exhibited the absorption characteristics of the Au metal. When the metal thickness was decreased, the unwanted color of the TCL was reduced. A photograph of the Au metal mesh with the line height of 10 nm fabricated on glass is displayed in Fig. 3(d).

Using this fabrication method, metal meshes composed of various kinds of metals, such as copper (Cu) and aluminum (Al), can be prepared (see ESI Fig. S1†). To produce Cu and Al meshes, it is only necessary to change the etching plasma and the corresponding oxides deposited on the CNTs.

Compared with commercial ITO that has a transmittance of almost 85% at 550 nm, the as-fabricated metal mesh composed of Au nanowires showed relatively poor performance in terms of transmittance. This was mainly because too many Au nanowires formed on the substrate greatly increased

the absorption of visible light. Therefore, as a fabrication technology with great flexibility, the density of SACNTs in the networks was decreased by a laser treatment process (LP). After the SACNT film was prepared on the suspended metal frame, LP was used to modify its morphology. A laser with a wavelength of 1.06  $\mu\text{m}$  was used to scan along the direction of the SACNTs at intervals of 0.1 mm. Fig. 4(a) compares a SACNT film before and after LP. LP effectively decreased the amount of CNTs in the treated area *via* the heat effect. The SACNT film was thinned periodically by LP, but the film remained free-standing. Correspondingly, the use of the modified SACNT film as an etching mask decreased the Au nanowire density of the metal mesh. Microscopy images of this metal mesh (Fig. 4(c)) revealed that laser treatment of the SACNT film etching mask produced an Au metal mesh with designated intervals. The inset shows a photograph of the as-fabricated mesh on glass. Compared with the mesh shown in Fig. 2(d), decreasing the density of the SACNT film resulted in fewer Au nanowires on the substrate. Fig. 4(b) shows that the transmittance of metal meshes fabricated from Au layers of various thicknesses using laser-treated SACNT etching masks was improved compared with that of the meshes mentioned before. In this case, for the metal mesh fabricated from an Au layer with a thickness of 10 nm, the transmittance at 550 nm was 87.5% with a sheet resistance of 78.2  $\Omega \square^{-1}$ , which is comparable to the properties of commercial ITO. Meanwhile, the resistance (transmittance at 550 nm) of Au meshes fabricated using LP SACNT films and Au layer thicknesses of 15, 20 and 25 nm was 11.5  $\Omega \square^{-1}$  (59.4%), 18.6  $\Omega \square^{-1}$  (71.7%) and 50.9  $\Omega \square^{-1}$  (82.6%), respectively. (The resistances and optical transmittances of Al and Cu LP metal meshes are shown in ESI Fig. S2†). Because treatment with a laser is highly flexible, various kinds of masks based on SACNT films could be realized (ESI Fig. S3†). The LP-treated masks could then be used to further modify the morphology of metal meshes (ESI Fig. S4†).

Fig. 4(d) plots the optical transmittance at 550 nm against the corresponding sheet resistance for various transparent conductive materials, including Au layers, ITO,<sup>31</sup> CNTs and graphene.<sup>9</sup> Note that the transmittance used here excludes the influence of the substrate. Compared with other techniques for TCL fabrication, the Au metal mesh obtained following LP treatment exhibits compatible performance.

Au metal meshes were also prepared on different kinds of substrates to demonstrate the scope of this fabrication method. Au layers with a thickness of 10 nm were deposited on a transparent tape and PET substrates instead of glass. The Au layers on these flexible substrates were etched in the same manner as on the rigid substrate. Au metal meshes with similar structures to that obtained on glass could also be prepared on the tape and PET substrates. Fig. 5(a) and (b) show that the tape and PET substrates became conductive after the fabrication of Au metal meshes on them, while maintaining their flexibility and transparency compared with the samples prepared on glass (Fig. 5(c)). Because there was no substrate selectivity in the etching process, it could be

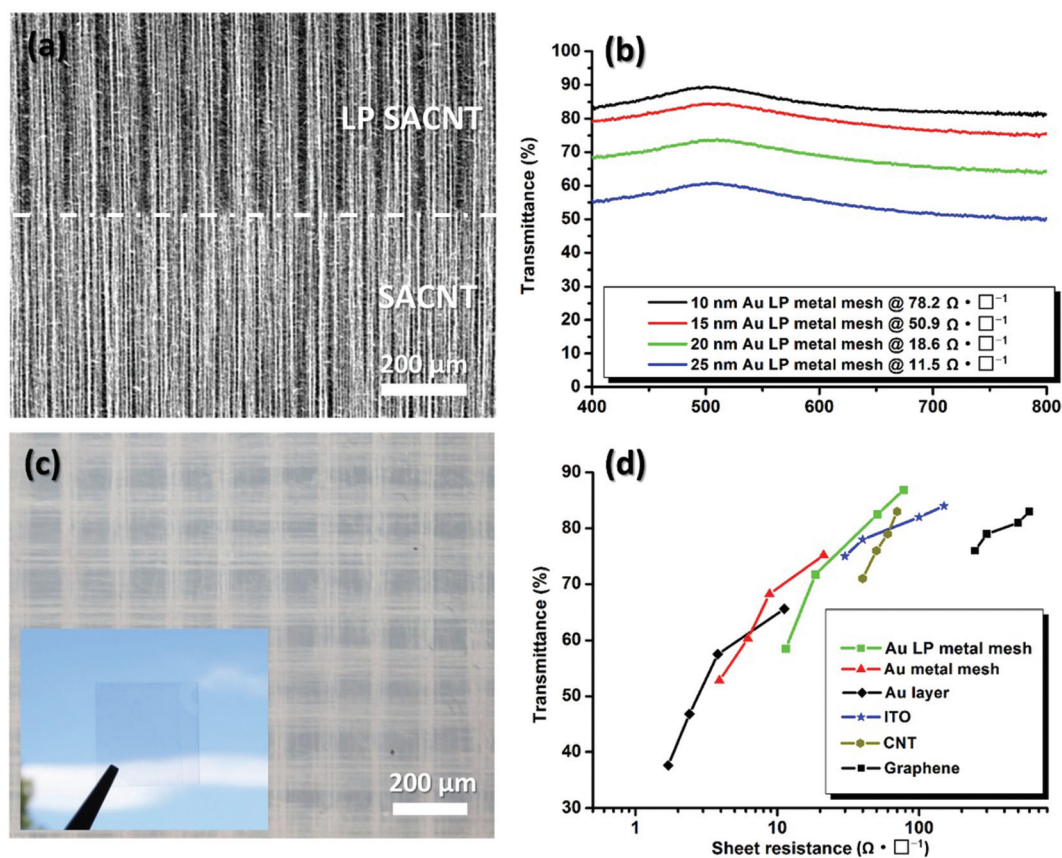


Fig. 4 (a) SEM image of a SACNT film with and without laser (LP) treatment. (b) Optical transmittance as a function of wavelength for Au metal meshes fabricated on glass substrates using LP-treated SACNT films. These metal meshes were fabricated from Au layers with thicknesses of 10, 15, 20 and 25 nm. (c) Microscopy image of an Au metal mesh fabricated on glass from a 10 nm Au layer and LP-treated SACNT etching mask. The inset is a photograph of the sample fabricated from a 10 nm Au layer on glass. (d) Comparison of sheet resistance against optical transmission at 550 nm for an Au layer, ITO, CNTs, graphene and samples in this work.

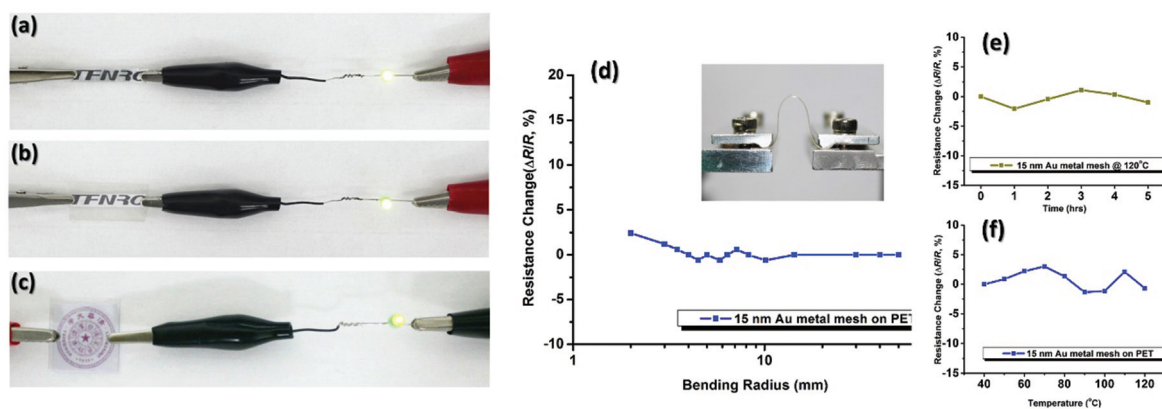


Fig. 5 Photographs of conductive layers on (a) tape, (b) PET and (c) glass substrates. (d) Resistance change of samples fabricated from a 15 nm Au layer on a flexible PET substrate against bending radius. (e) Resistance of an Au mesh prepared using an Au layer with a thickness of 15 nm on a PET substrate over time maintained at 120 °C. (f) Resistance of an Au mesh fabricated from a 15 nm Au layer on a PET substrate with increasing temperature.

carried on various substrates with a deposited metal layer, which makes this approach have broad commercial application prospects.

To examine the mechanical durability of the Au metal meshes, a sample was fabricated on a PET substrate using a 15 nm Au layer. Fig. 5(d) plots the sheet resistance of the Au

metal mesh as a function of bending radius determined with the measurement setup shown in the inset. The film could be bent to a radius of 2 mm without any obvious degradation of electrical conductivity. For commercial TCL applications, the long-term stability of the products under some extreme conditions remains an important factor.<sup>13</sup> For example, TCL materials used outdoors in solar cells require stable performance when heated by sunlight. Therefore, we heated the Au metal mesh fabricated from a 15 nm Au layer on PET mentioned above at 120 °C for 5 h to examine the variation in resistance at high temperatures. Resistance was measured every 60 min and the measurement process was executed as soon as possible to avoid the influence of sudden changes of temperature on the resistance. Fig. 5(e) reveals that the resistance change of the sample remained around 2–3% for 5 h at 120 °C, which demonstrates the good stability of the product at high temperatures. The resistance of the same sample during heating from 40 to 120 °C in increments of 10 °C every 60 min was also measured (Fig. 5(f)). The resistance of the mesh remained stable as the temperature was increased. The excellent stability of the metal meshes towards temperature could be attributed to the high thermal stability of the metals (ESI Fig. S5†). Furthermore, in metal nanowire networks fabricated by traditional methods, the junction resistance between the nanowires appears to be the main reason for their degradation. In contrast, the metal meshes fabricated here did not possess junction resistance. This is why the as-fabricated metal meshes remained stable for a relatively long time under extreme conditions.

## Conclusions

In conclusion, SACNT networks were proven to be effective as etching masks to fabricate several kinds of metal meshes on both rigid and flexible substrates for the first time. With the advantage of suspended preparation on a large-scale, various kinds of metal oxides could be deposited on the SACNT networks, which ensure their availability as masks in different etching processes. Metal meshes fabricated from Au, Cu, and Al demonstrated suitable properties for use as TCLs. The transmittance of the Au mesh reached 87.5%, and its resistance was comparable to that of current commercial TCL materials. Furthermore, the sheet resistance of the metal meshes was lowered by the lack of junction resistance in the interconnected metal nanostructures. The resistance of the metal mesh remained stable at high temperatures, demonstrating that it is durable under extreme conditions. An Au metal mesh on a flexible substrate could be bent down to a radius of 2 mm with no obvious degradation of electrical conductivity.

## Conflict of interest

The authors declare no competing financial interest.

## Acknowledgements

This work was financially supported by the National Basic Research Program of China (2012CB932301) and the Natural Science Foundation of China (90921012, 11574171).

## References

- H. Cheong, R. E. Triambulo, G. Lee, I. Yi and J. Park, *ACS Appl. Mater. Interfaces*, 2014, **6**, 7846–7855.
- M. G. Kang and L. J. Guo, *Adv. Mater.*, 2007, **19**, 1391–1396.
- S. Bae, H. Kim, Y. Lee, X. Xu, J. Park, Y. Zheng, J. Balakrishnan, T. Lei, H. Ri Kim, Y. I. Song, Y. Kim, K. S. Kim, B. Özyilmaz, J. Ahn, B. H. Hong and S. Iijima, *Nat. Nanotechnol.*, 2010, **5**, 574–578.
- M. Kang, T. Xu, H. J. Park, X. Luo and L. J. Guo, *Adv. Mater.*, 2010, **22**, 4378–4383.
- C. Zhang, D. Zhao, D. Gu, H. Kim, T. Ling, Y. R. Wu and L. J. Guo, *Adv. Mater.*, 2014, **26**, 5696–5701.
- R. Bel Hadj Tahar, T. Ban, Y. Ohya and Y. Takahashi, *J. Appl. Phys.*, 1998, **83**, 2631.
- C. G. Granqvist, *Thin Solid Films*, 2014, **564**, 1–38.
- A. Kumar and C. Zhou, *ACS Nano*, 2010, **4**, 11–14.
- D. S. Hecht, L. Hu and G. Irvin, *Adv. Mater.*, 2011, **23**, 1482–1513.
- L. Hu, D. S. Hecht and G. Grüner, *Appl. Phys. Lett.*, 2009, **94**, 81103.
- L. Hu, H. Wu and Y. Cui, *MRS Bull.*, 2011, **36**, 760–765.
- C. Niu, *MRS Bull.*, 2011, **36**, 766–773.
- K. Ellmer, *Nat. Photonics*, 2012, **6**, 809–817.
- P. B. Catrysse and S. Fan, *Nano Lett.*, 2010, **10**, 2944–2949.
- P. Hsu, S. Wang, H. Wu, V. K. Narasimhan, D. Kong, H. Ryoung Lee and Y. Cui, *Nat. Commun.*, 2013, **4**.
- J. van de Groep, P. Spinelli and A. Polman, *Nano Lett.*, 2012, **12**, 3138–3144.
- S. Tawfick, M. De Volder, D. Copic, S. J. Park, C. R. Oliver, E. S. Polsen, M. J. Roberts and A. J. Hart, *Adv. Mater.*, 2012, **24**, 1628–1674.
- H. Wu, D. Kong, Z. Ruan, P. Hsu, S. Wang, Z. Yu, T. J. Carney, L. Hu, S. Fan and Y. Cui, *Nat. Nanotechnol.*, 2013, **8**, 421–425.
- T. Gao, B. Wang, B. Ding, J. Lee and P. W. Leu, *Nano Lett.*, 2014, **14**, 2105–2110.
- B. Han, K. Pei, Y. Huang, X. Zhang, Q. Rong, Q. Lin, Y. Guo, T. Sun, C. Guo, D. Carnahan, M. Giersig, Y. Wang, J. Gao, Z. Ren and K. Kempa, *Adv. Mater.*, 2014, **26**, 873–877.
- K. Jiang, Q. Li and S. Fan, *Nature*, 2002, **419**, 801.
- P. Liu, Y. Wei, K. Liu, L. Liu, K. Jiang and S. Fan, *Nano Lett.*, 2012, **12**, 2391–2396.
- K. Jiang, J. Wang, Q. Li, L. Liu, C. Liu and S. Fan, *Adv. Mater.*, 2011, **23**, 1154–1161.
- A. Sandhu, *Nat. Nanotechnol.*, 2009, **4**, 398–399.
- C. Feng, K. Liu, J. Wu, L. Liu, J. Cheng, Y. Zhang, Y. Sun, Q. Li, S. Fan and K. Jiang, *Adv. Funct. Mater.*, 2010, **20**, 885–891.

- 26 K. Liu, Y. Sun, P. Liu, X. Lin, S. Fan and K. Jiang, *Adv. Funct. Mater.*, 2011, **21**, 2721–2728.
- 27 Y. Wei, P. Liu, K. Jiang and S. Fan, *Nano Lett.*, 2012, **12**, 2548–2553.
- 28 X. Zhang, K. Jiang, C. Feng, P. Liu, L. Zhang, J. Kong, T. Zhang, Q. Li and S. Fan, *Adv. Mater.*, 2006, **18**, 1505–1510.
- 29 W. S. Yun, J. Kim, K. Park, J. S. Ha, Y. Ko, K. Park, S. K. Kim, Y. Doh, H. Lee, J. Salvétat and L. Forró, *J. Vac. Sci. Technol., A*, 2000, **18**, 1329.
- 30 A. V. Krasheninnikov, K. Nordlund and J. Keinonen, *Appl. Phys. Lett.*, 2002, **81**, 1101.
- 31 Sigma-Aldrich, <http://www.sigmaaldrich.com/united-states.html>.
- 32 Y. Jin, Q. Li, M. Chen, G. Li, Y. Zhao, X. Xiao, J. Wang, K. Jiang and S. Fan, *Small*, 2015, **11**, 4111.
- 33 D. R. Lide, *CRC Handbook of Chemistry and Physics*, CRC, Press, Boca Raton, FL, 90th edn, 2009.